Contents lists available at ScienceDirect

Saudi Pharmaceutical Journal

Original article

Antimicrobial activity of the biogenically synthesized core-shell Cu@Pt nanoparticles

Renata Dobrucka [a],*, Jolanta Dlugaszewska [b]

[a] *Department of Industrial Products Quality and Ecology, Faculty of Commodity Science, Poznan University of Economics, al. Niepodległości 10, 61-875 Poznan, Poland*
[b] *Department of Genetics and Pharmaceutical Microbiology, Poznan University of Medical Sciences, 10 Fredry Street, 61-701 Poznan, Poland*

ABSTRACT

The interest in the biological synthesis of mono metal nanoparticles has been visible for years. As more attention is also given to the biological methods of synthesizing bimetallic nanoparticles, this work used the *Agrimoniae herba* extract in order to obtain bimetallic core-shell Cu@Pt nanoparticles. The formed core-shell Cu@Pt nanoparticles were characterized by Ultraviolet–Visible (UV–vis), Fourier Transform-Infrared (FT-IR), Scanning electron microscopy (SEM), Transmission Electron Microscopy (TEM) and Atomic Force Microscopy (AFM) measurements. The obtained core-shell Cu@Pt nanoparticles were analysed in terms of their antibacterial activity. It was discovered that the synthesized nanoparticles exhibited maximum activity against gram-negative bacteria *E. coli* ATCC 25922, *S. aureus* ATCC 25923, and *P. aeruginosa* NCTC 6749. The core-shell Cu@Pt nanoparticles also exhibited activity against the yeast *C. albicans* ATCC 10231 and dermatophytes *T. mentagrophytes* ATCC 9533.

© 2018 The Authors. Production and hosting by Elsevier B.V. on behalf of King Saud University. This is an open access article under the CC BY-NC-ND license (http://creativecommons.org/licenses/by-nc-nd/4.0/).

1. Introduction

Nanotechnology is one of the fastest-growing fields of science. Nanomaterials have diverse physico-chemical properties that enable their usage in a wide range of innovative applications (Rackauskas et al., 2009; Salata, 2004; Gwinn and Vallyathan, 2006). Therefore, they have become part of a commercial revolution that has resulted in the production of hundreds of new products. Especially interesting solutions are created by combining metal nanoparticles. They usually provide novel or enhanced properties, which are not exhibited by their individual components (Zhong et al., 2010; Feng et al., 2010). Recently, bimetallic nanoparticles have attracted greater attention than monometallic nanoparticles from both scientific and technological viewpoints due to their potential unique electronic, optical, catalytic or photocatalytic properties, which are absent in the coincident monometallic nanoparticles (Zaleska-Medynska et al. 2016).

The literature presents numerous examples of obtaining bimetallic nanoparticles using physical and chemical methods, which are usually expensive as well as potentially hazardous to the environment and organisms. The present trend moves towards the departure from the traditional methods of synthesizing nanoparticles and the search for a new alternative. One of such alternatives is the biological synthesis of metal nanoparticles. In the biological methods, the use of plant extracts has certain advantages: they are easily available, safe to handle, and they possess a broad viability of metabolites. Moreover, it has been found that plant extracts act both as reducing and capping agents in the process of synthesizing nanoparticles (Nasrollahzadeh et al., 2016).

The biological method is widely used in order to obtain monometallic nanoparticles, including Au, Ag or Pt. There are only few examples of obtaining bimetallic nanoparticles by means of biological synthesis. Therefore, in order to obtain the core-shell Cu@Pt nanoparticles, this work used the *Agrimoniae herba* extract. *Agrimonia eupatoria* (Rose Family: Rosaceae) is a medicinal plant with a wide range of applications. It is known as agrimony in the English literature, and it is used in folkloric medicine to treat various ailments (Duke, 2002). The raw material is obtained from the ground parts of the plant collected in the period of anthesis. It has contracting and anti-inflammatory properties, and it is rich in chemical constituents (flavonoids, tannins, aromatic acids, triterpenes, coumarins, terpenoids, glycosides, and vitamins B and K (Xu et al., 2005). Due to the presence of numerous biologically

Production and hosting by Elsevier

active substances, it was decided to use *Agrimoniae herba* extract in order to synthesize the core-shell Cu@Pt nanoparticles.

2. Materials and methods

The upper parts of shoots and the leaves of *Agrimoniae herba* were collected in Wielkopolska region (Poland) (52.320°N, 17.579°E) in June 2016. *A. herba* was washed with deionized water, dried in a dark place (in temperature up to about 40° C) and powdered. All chemicals used this article were purchased in Sigma-Aldrich (Poland). They were of analytical grade and used without further purification.

2.1. Synthesis of Cu@Pt nanoparticles

1 g of powdered *A. herba* was put into 250 ml of the aqueous solution of ethanol in the 1:1 ratio. The solution was heated and stirred vigorously for 50 min. at 80 °C. Then, the extract was filtered through Whatman's No. 1 filter paper and set aside. During the second stage, the solutions of K_2PtCl_6 0.40 [mM] and $CuSO_4$ 0.90 [mM] were combined in the 1:1 ratio. The obtained solution was mixed with the extract, and then stirred for 24 h at 65 °C. The UV-absorption spectrum of the synthesized Cu@Pt nanoparticles was monitored after 4 h, 8 h, 16 h and 24 h.

2.2. Characterization of Cu@Pt nanoparticles

In this work, the UV–VIS absorption spectra of the synthesized Cu@Pt nanoparticles were obtained from a spectrophotometer Cary E 5000 in the range of 300–800 nm using a quartz cell with 10 mm of optical path length (Agilent, USA). FTIR spectra of the samples were measured using Perkin-Elmer Spectrum 1000, in attenuated total reflection mode, and using the spectral range of 4000–380 cm^{-1}. The study also used one instrument in the diffuse reflectance mode at the resolution of 4 cm^{-1} in KBr pellets (Perkin Elmer, USA). The obtained Cu@Pt nanoparticles were characterized using an Atomic Force Microscope (Agilent, USA). The size and morphology of the synthesized Cu@Pt nanoparticles were characterized using a Transmission Electron Microscope JEOL JEM 1200 EXII, operating at 200 kV. Moreover, we used a Scanning Electron Microscope (HR SEM) Helios NanoLab 660 (FEI). SEM imaging was performed in the immersion mode (Thermo Fisher Scientific, USA).

2.3. Antimicrobial activity of Cu@Pt nanoparticles

The microorganisms used in the study were standard strains of *Staphylococcus aureus* NCTC 4163, *Escherichia coli* ATCC 25922, *Pseudomonas aeruginosa* NCTC 6749, *Candida albicans* ATCC 10231, *Aspergillus fumigatus* ATCC 204305 and *Trichophyton mentagrophytes* ATCC 9533. The strains were obtained from the National Collection of Type Cultures (NCTC) and from the American Type Culture Collection (ATCC). The bacterial and yeast (*C. albicans*) strains were stored in Microbank cryogenic vials (ProLabDiagnostics, Canada) at −70 °C ± 10 °C. The bacteria were cultured aerobically in brain-heart infusion broth (BHI; OXOID, UK) at 36 °C ± 1 °C for 20 h and *C. albicans* cultures were grown in Sabouraud dextrose broth (SDB; OXOID, UK) at 36 °C ± 1 °C for 20 h. The bacteria and *C. albicans* were harvested by centrifugation (3000 rpm for 15 min), re-suspended in 10 mM PBS, pH, 7.0 (Sigma-Aldrich, USA), and then diluted in a suitable medium to obtain the desired concentrations.

Filamentous fungi were inoculated on Sabouraud dextrose agar (Merck, Germany) and incubated at 34 °C for 5–8 days (*A. fumigatus*) and for 3 weeks (*T. mentagrophytes*) for adequate sporulation.

After incubation, cultures were covered with sterile 0.9% NaCl solution supplemented with 0.1% Tween 80, carefully rubbed with a sterile cotton swab, and transferred to a sterile flask. Suspensions were homogenized and filtered. The number of spores in the suspension was determined using the serial dilution method. Before using, the suspension was diluted in 0.9% NaCl to obtain the desired number of spores in the suspension.

2.3.1. Well diffusion method

The antimicrobial activity was determined by means of the well diffusion method according to Valgas et al. (2007). Mueller-Hinton Agar (MHA; OXOID, UK) and Sabouraud dextrose agar (SDA; OXOID, UK) plates were inoculated with a microbe suspension containing: bacteria and *C. albicans* – about 10^7 CFU/mL, *A. fumigatus* and *T. mentagrophytes* – about 5.0×10^6 CFU/mL. Next, wells with the diameter of 7 mm were punched into the medium. Then, 100 μl aliquots of the tested core-shell Cu@Pt nanoparticles were dispensed into each well. For each microbial strain controls were maintained where pure extract was used instead of the core-shell Cu@Pt nanoparticles. The plates were incubated at 36 °C ± 1 °C for 18 h – bacteria and *C. albicans*, for 48 h – *A. fumigatus*, and for 5 days – *T. mentagrophytes*. After incubation, the inhibition zones were measured. Every experiment was carried out in triplicate, and the result represented the average of three independent experiments.

2.3.2. Determination of MIC, MBC and MFC

In this study, the minimal inhibitory concentration (MIC), minimal bactericidal and fungicidal concentration (MBC, MFC) values of the core-shell Cu@Pt nanoparticles were evaluated by the broth microdilution method using 96-well microtiter plates in accordance with the EUCAST (European Committee on Antimicrobial Susceptibility Testing) guidelines with modifications.

The core-shell Cu@Pt nanoparticles and the pure extract were diluted to give the final concentration of 80%, 40%, 20%, 10%, 5%, 2.5%, and 1.25%. Aliquots of 100 μl of each dilution were distributed in 96-well plates (Kartell, Italy), as well as a sterility control (containing the tested substance and culture broth) and a growth control (containing culture broth without the tested substance). The test and growth control wells were inoculated with 100 μl of a standardized microbial suspension of test microorganisms to obtain a final concentration about 5×10^5 CFU/mL – bacteria and about 2.5×10^5 CFU/mL – fungi. The plates were incubated at 34 °C for 18 h – bacteria and *C. albicans*, for 48 h – *A. fumigatus*, and for 5 days – *T. mentagrophytes*. The MIC was defined as the lowest concentration at which no visible growth (no turbidity) was observed. After performing the MIC test and recording the MIC end point, every well that demonstrated no growth (concentration equal to and greater than the MIC) was subcultured onto an agar medium: Typcase soy agar (TSA; OXOID, UK) – bacteria; SDA – fungi. The plates were incubated at 34 °C for 18 h – bacteria and *C. albicans*, for 48 h – *A. fumigatus*, and for 5 days – *T. mentagrophytes*. The minimal bactericidal concentration (MBC) and the minimal fungicidal concentration (MFC) were defined as the lowest concentration at which no growth was observed

3. Results and discussion

3.1. Uv–visible absorption of Cu@Pt nanoparticles

The optical properties of the synthesized nanoparticles were measured by means of the UV–Vis spectroscopy. The UV–Vis absorption spectra were measured over a range of 300–800 nm with spectrophotometer Cary E 500 using a quartz cell with 10 mm of optical path length. Fig. 1 presents the UV–visible spectra
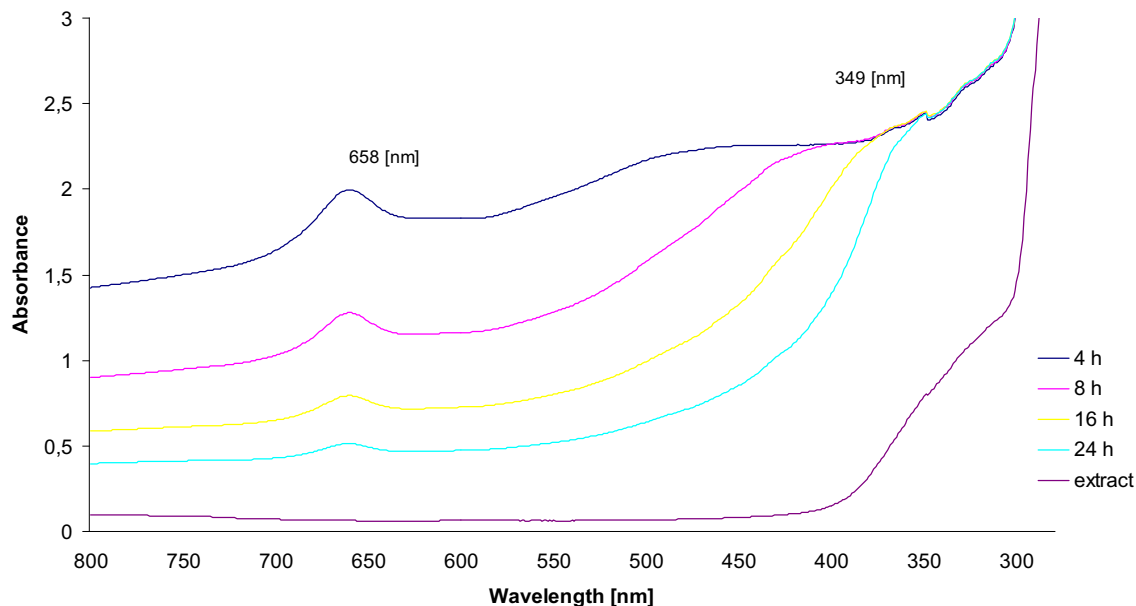
Fig. 1. UV–Visible spectra of Cu@Pt nanoparticles synthesized using *Agrimoniae herba* extract.

of Cu@Pt nanoparticles and the *A. herba* extract. The absorbance was read after 4 h, 8 h, 16 h and 24 h after mixing the solutions of K_2PtCl_6 and $CuSO_4$ with the extract prepared earlier in the 1:1 ratio. After 4 and 8 h, there were clearly visible peaks at 658 nm and 349 nm. They confirmed the presence of Pt^{4+} and Cu^{2+} ions in the solution. After 16 h, the intensity of two peaks was not that clear. After 24 h of reaction at 65 °C, the absorption peaks disappeared, which was the evidence of the complete reduction of Pt^{4+} and Cu^{2+} ions, and the formation of Cu@Pt nanoparticles.

3.2. FTIR analysis of Cu@Pt nanoparticles

The FTIR spectra of Cu@Pt nanoparticles synthesized using *A. herba* extract showed the major absorption bands at 3308 cm^{-1}, 2112 cm^{-1}, 1634 cm^{-1}, 1044 cm^{-1}, 422 cm^{-1}, 411 cm^{-1}, 402 cm^{-1}, and 394 cm^{-1} (Fig. 2). The peak which appeared at 3308 cm^{-1} is related to O—H stretching (intramolecular hydrogen bonded OH). The peak which appeared at 2112 cm^{-1} may indicate the presence of alkynes group. The most intense band at 1634
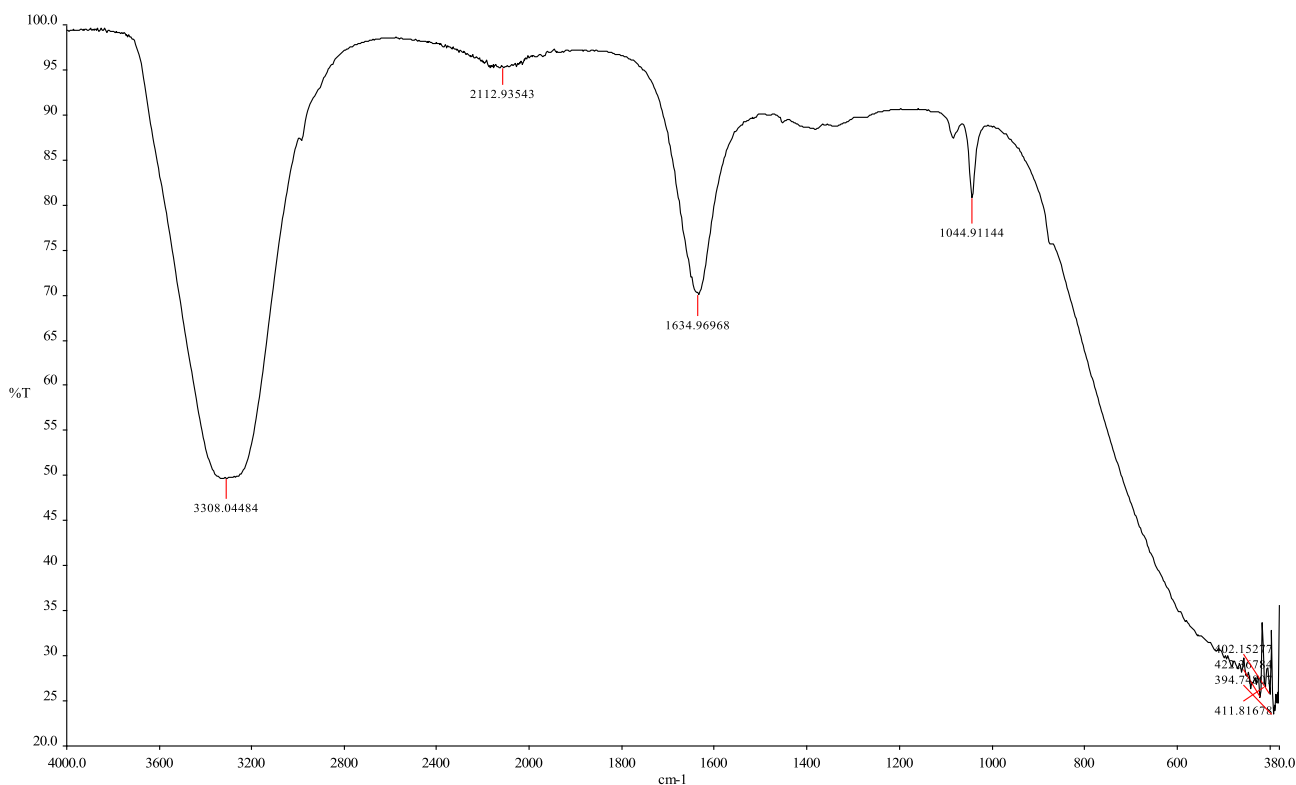
Fig. 2. FTIR spectra of Cu@Pt nanoparticles synthesized using *Agrimoniae herba* extract.

cm^{-1} represents vibrations C=O, typical for the structure of flavonoids. The absorption peak at 1044 cm^{-1} was assigned for C—O—C and the secondary —OH of the phenolic group. The absorption bands at 422 cm^{-1}, 411 cm^{-1}, 402 cm^{-1} and 394 cm^{-1} indicated the formation of metal–biomolecules present in the extract.

The studies confirm the presence of active compounds in *A. herba*. It has been assumed that bioactive compounds act as the reducing and capping agents of Cu@Pt nanoparticles. *A. herba* contains tannins (about 5%): mainly catechinic tannins and elagotanoids, flavones (such as luteolin, apigenin), flavonols (such as
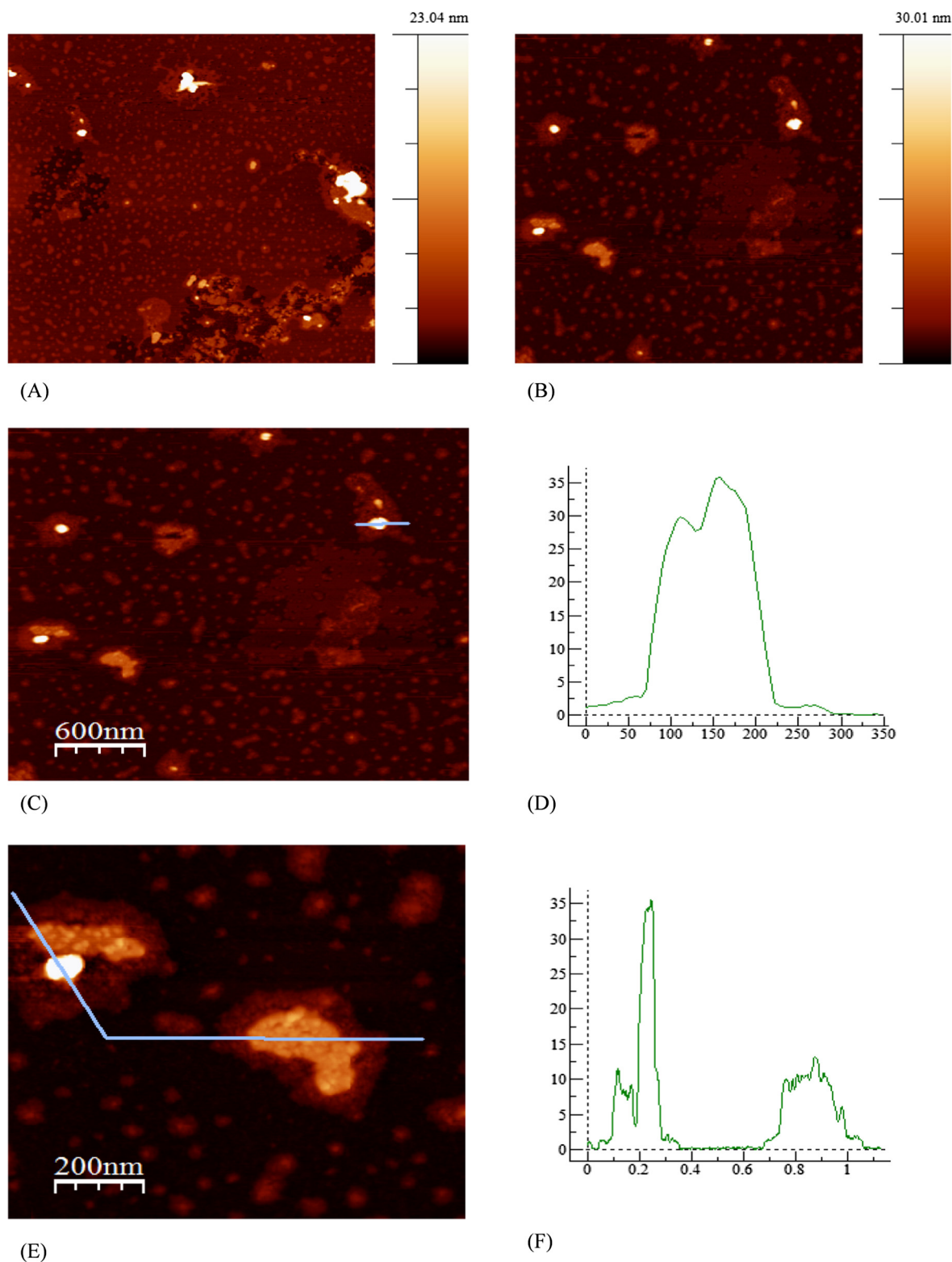
Fig. 3. AFM images of Cu@Pt nanoparticles synthesized using *Agrimoniae herba* extract.

kaempferol), and organic acids (Matławska, 2008). Depending on the stage of growth and development, it contains from 4 to 10% ellagic tannins, catechinic tannins, including gallocatechins. Tannins impede the peroxidation of lipids, they scavenge free radicals, and they inhibit the formation of superoxide ions. Flavonoids exhibit a variety of biological and pharmacological properties, including antiulcer, antiallergic, cardiovascular protection, anticancer, antiviral, and anti-inflammatory potential (Dehghan et al., 2007). Luteolin present in *A. herba* has high antioxidant properties

(Leung et al., 2006). Similarly high antioxidant activity is exhibited by apigenin. It was proven, among others, by the studies conducted by Majewska et al. (2011). In the studies, the author examined the antioxidant potential of flavonoids. Among the tested flavonoids, the highest level of radical scavenging properties at all concentrations was exhibited by quercetin, and then, respectively, by luteolin, rhamnetin, isorhamnetin, and apigenin. The high antioxidant potential of flavonoids stems mainly from their chemical structure, which has an important impact on the radical
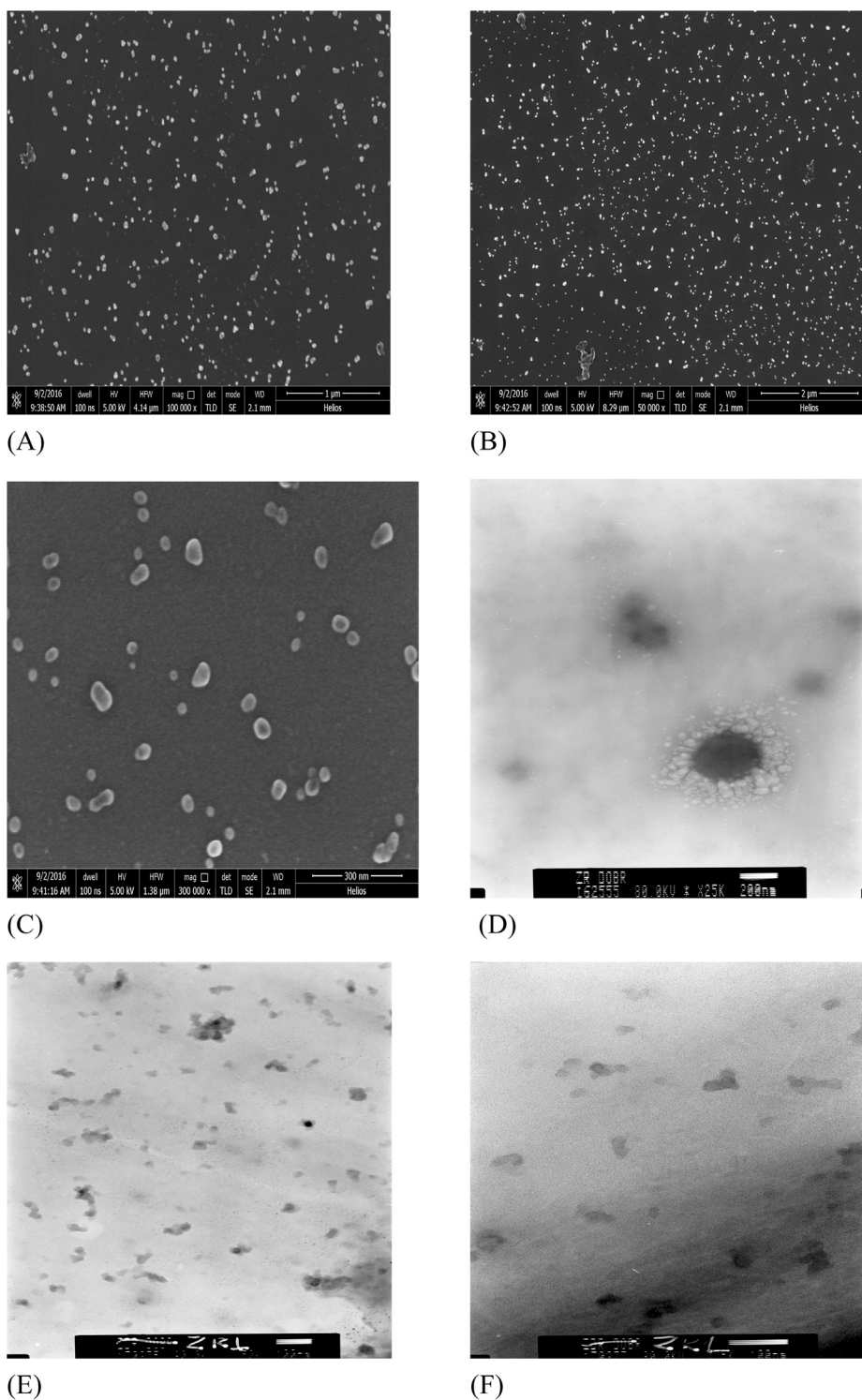
Fig. 4. SEM images of Cu@Pt nanoparticles synthesized using *Agrimoniae herba* extract.

Table 1
Antimicrobial activity of the biogenically synthesized core-shell Cu@Pt nanoparticles and *Agrimoniae herba* extract.

Microorganisms	Zone of inhibition (mm) ±SD against bacterial and fungal strains	
	The core-shell Cu@Pt nanoparticles	Agrimoniae herba extract
Staphylococcus aureus ATCC 25923	11.0 ± 0.0	10.0 ± 0.0
Escherichia coli ATCC 25922	12.7 ± 0.6	7.0 ± 0.0
Pseudomonas aeruginosa NCTC 6749	10.0 ± 0.0	7.0 ± 0.0
Candida albicans ATCC 10231	10.3 ± 0.6	7.0 ± 0.0
Aspergillus fumigatus ATCC 20430	7.7 ± 0.6	7.0 ± 0.0
Trichophyton mentagrophytes ATCC 9533	10.3 ± 0.6	7.0 ± 0.0

scavenging activity. The more hydroxyl moieties, the higher the antioxidant activity. *A. herba* also contains flavonols (such as kaempferol). Kaempferol exhibits high antioxidant properties. Furthermore, the studies conducted by Mirjana et al. (2016) proved that water, diethyl ether, acetone, and ethanol extracts of *Agrimonia eupatoria L.* showed a very strong antioxidant activity.

3.3. AFM analysis of Cu@Pt nanoparticles

The examination by means of the Atomic Force Microscopy (AFM) made it possible to determine the size of the obtained Cu@Pt nanoparticles. The study confirmed the presence of 30–35 nm Cu@Pt nanoparticles and 10 nm particles. Fig. 3 presents the AFM images of Cu@Pt nanoparticles synthesized using the *A. herba* extract where (A) the topography is 5 μm × 5 μm, (B) the topography is 3 μm × 3 μm, (C) the topography is 3 μm × 3 μm with selected section, (D) the intersection (for Z = 35) is 3 μm × 3 μm, (E) the topography is 1 μm × 1 μm with selected section, (F) the intersection (for Z = 35) is 1 μm × 1 μm.

3.4. SEM and TEM analysis of Cu@Pt nanoparticles

The size of Cu@Pt nanoparticles was measured also by means of Scanning Electron Microscopy. There were observed very small (about 30 nm) Cu@Pt nanoparticles, and the majority of them were spherical. The size of nanoparticles determined by means of SEM was consistent with the results obtained by means of Atomic Force Microscopy. The nanoparticles were examined with the use of Transmission Electron Microscopy because this method made it possible to investigate whether or not the Cu nanoparticles are covered with shell material. It was observed that the surface of

(A1)   (B1)   (A2)   (B2)

(A3)   (B3)   (A4)   (B4)
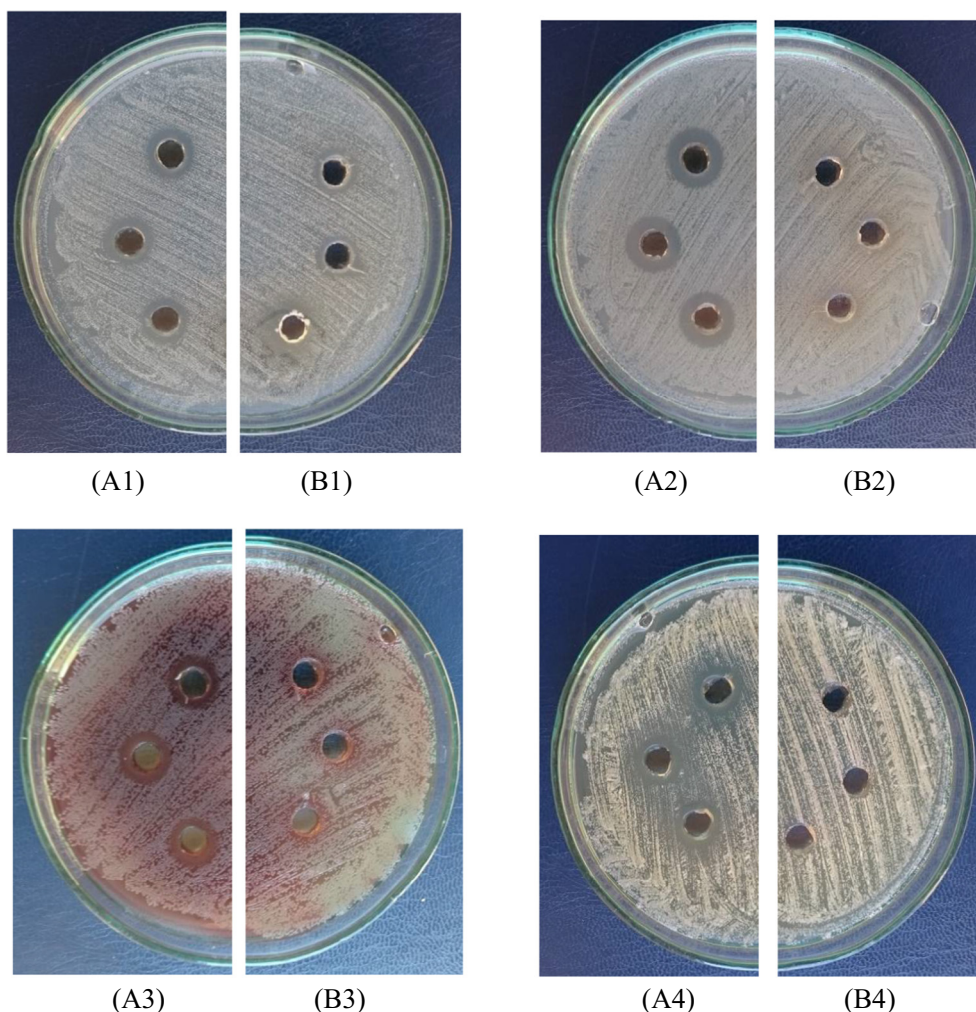
Fig. 5. Antimicrobial effect of (A1–A4) the Cu@Pt nanoparticles and (B1–B4) the *Agrimoniae herba* extract against (A1, B1) *Staphylococcus aureus* ATCC 25923; (A2, B2) *Escherichia coli* ATCC 25922; (A3, B3) *Pseudomonas aeruginosa* NCTC 6749 and (A4 and B4) *Candida albicans* ATCC 10231.

Table 2
MIC, MBC and MFC value of the biogenically synthesized core-shell Cu@Pt nanoparticles and *Agrimoniae herba* extract.

| Microorganisms | Minimal Inhibitory Concentration, Minimal Bactericidal Concentration and Minimal Fungicidal Concentration value (%) ±SD | | | |
| | The core-shell Cu@Pt nanoparticles | | Agrimoniae herba extract | |
	MIC	MBC/MFC	MIC	MBC/MFC
Staphylococcus aureus ATCC 25923,	16.7 ± 5.8	33.3 ± 11.6	26.7 ± 11.6	>80
Escherichia coli ATCC 25922	40.0 ± 0.0	40.0 ± 0.0	>80	>80
Pseudomonas aeruginosa NCTC 6749	40.0 ± 0.0	53.3 ± 23.1	>80	>80
Candida albicans ATCC 10231	40.0 ± 0.0	66.7 ± 23.1	>80	>80
Aspergillus fumigatus ATCC 20430	53.3 ± 23.1	53.3 ± 23.1	>80	>80
Trichophyton mentagrophytes ATCC 9533	26.7 ± 11.6	26.7 ± 11.6	>80	>80

the spherical core of Cu was covered with a Pt layer. Fig. 4 presents SEM images of Cu@Pt nanoparticles with magnification (A) 100,000×, (B) 50,000×, (C) 300,000× and TEM images where the scale bar is (D) 200 nm and 100 nm (E), (F).

3.5. Antimicrobial activity studies of Cu@Pt nanoparticles

According to Esteban-Cubillo et al., (2006), the core-shell composite has many advantages as antibacterial agent, such as high antibacterial activity, low toxicity, chemical stability and long lasting action period. Also, this study evaluated the antimicrobial activity of the biogenically synthesized core-shell Cu@Pt nanoparticles. In the literature there are examples of the synthesis of bimetallic Pt-Cu nanoparticles (Toshima and Wang, 1994; Obuchi et al., 1993; Odenbrand et al., 1999; Thandavarayan et al., 2012). However, studies do not evaluate the antimicrobial activity of Pt-Cu nanoparticles. There are works on microbial activity bimetallic core -shell nanaoparticles metals such as Ag@SiO$_2$ (Otari et al., 2016), Au@Ag (Huo et al., 2014) or Ag@TiO$_2$ (Dhanalekshmi and Meena, 2014). Using the agar dilution method, it was observed that the Cu@Pt nanoparticles showed various degree of activity against bacterial and fungal standard strains (Table 1).

The Cu@Pt nanoparticles exhibited maximum activity against gram-negative bacteria *E. coli* ATCC 25922, gram-positive bacteria *S. aureus* ATCC 25923 and gram-negative bacteria *P. aeruginosa NCTC 6749* as well as yeast *C. albicans* ATCC 10231, and dermatophytes *T. mentagrophytes* ATCC 9533. The nanoparticles did not exhibit activity against moulds *A. fumigatus* ATCC 20430. However, it should be noted that the *A. herba* extract also inhibited the growth of *S. aureus* ATCC 25923. The results are presented in Fig. 5. This Figure presents antimicrobial activity of the Cu@Pt nanoparticles and the *Agrimoniae herba* extract against *Staphylococcus aureus* ATCC 25923, *Escherichia coli* ATCC 25922, *Pseudomonas aeruginosa* NCTC 6749 and *Candida albicans* ATCC 10231. Fig. 5 (A1-A4) shows antimicrobial effect of the Cu@Pt nanoparticles and the *A. herba* extract (Fig. 5 B1-B4).

The present study measured the minimal inhibitory, bactericidal and fungicidal concentrations of the core-shell Cu@Pt nanoparticles against standard strains of gram-positive and gram-negative bacteria and fungi (Table 2). It was demonstrated that the tested Cu@Pt nanoparticles inhibited the growth of all microbes used in the study. The most sensitive strains were *S. aureus* ATCC 25923 and *T. mentagrophytes* ATCC 9533 but the control study revealed that the inhibition effect against *S. aureus* was also observed with the *A. herba* extract. The inhibition and biocidal effects on the remaining microorganism were observed at the concentration ranging from 40.0 ± 0.0% to 53.3 ± 23.1% and from 40.0 ± 0.0% to 66.7 ± 23.1% respectively. According to the observations, the obtained results were not affected by the *A. herba* extract used for preparation of the tested compound.

4. Conclusion

In this paper, we have reported the biogenically synthesized core-shell Cu@Pt nanoparticles. The bimetallic core-shell Cu@Pt nanoparticles were obtained using the *A. herba* extract. The assessment of the optical properties, size and shape of the nanoparticles was carried out by means of such methods as: UV–vis, FT-IR, SEM, TEM and AFM. The AFM examination confirmed the presence of Cu@Pt nanoparticles sized 30–35 nm. The TEM examination confirmed the presence of bimetallic Cu@Pt nanoparticles where the surface of the spherical core of Cu was covered with a Pt layer.

The study of antibacterial activity conducted using the agar dilution method indicated that the Cu@Pt nanoparticles showed various degrees of activity against bacterial and fungal standard strains. The Cu@Pt nanoparticles exhibited maximum activity against gram-negative bacteria *E. coli* ATCC 25922, gram-positive bacteria *S. aureus* ATCC 25923, and gram-negative bacteria *P. aeruginosa* NCTC 6749, as well as yeast *C. albicans* ATCC 10231 and dermatophytes *T. mentagrophytes* ATCC 9533. The nanoparticles did not exhibit any activity against moulds *A. fumigatus* ATCC 20430. The results are consistent with the results obtained by determining the minimal inhibitory concentration (MIC) and the minimal bactericidal and fungicidal concentration (MBC, MFC). *S. aureus* ATCC 25923 and *T. mentagrophytes* ATCC 9533 were the strains that exhibited the greatest sensitivity to the core-shell Cu@Pt nanoparticles.

Conflict of interest

The authors declare that they have no conflict of interest.

References

Dehghan, G., Shafiee, A., Ghahremani, M.H., Ardestani, S.K., Abdollahi, M., 2007. Antioxidant potential of various extracts from *Ferula szovitsiana*. in relation to their phenolic content. Pharm. Biol. 45 (9), 691–699.

Dhanalekshmi, K.I., Meena, K.S., 2014. Comparison of antibacterial activities of $Ag@TiO_2$ and $Ag@SiO_2$ core-shell nanoparticles. Spectrochim. Acta Part A: Mol. Biomol. Spectrosc. 128, 887–890.

Duke, J.A., 2002. Handbook of medicinal herbs. CRC Press.

Esteban-Cubillo, A., Pecharromán, C., Aguilar, E., Santarén, J., Moya, J.S., 2006. Antibacterial activity of copper monodispersed nanoparticles into sepiolite. J. Mater. Sci. 41 (16), 5208–5212.

Feng, L., Gao, G., Huang, P., Wang, K., Wang, X., Luo, T., Zhang, C., 2010. Optical properties and catalytic activity of bimetallic gold-silver nanoparticles. Nano Biomed. Eng. 2 (4), 258–267.

Gwinn, M.R., Vallyathan, V., 2006. Nanoparticles: health effects—pros and cons. Environ. Health Perspect. 114 (12), 1818.

Huo, D., He, J., Li, H., Yu, H., Shi, T., Feng, Y., Hu, Y., 2014. Fabrication of Au@ Ag core–shell NPs as enhanced CT contrast agents with broad antibacterial properties. Colloids Surf. B: Biointerfaces 117, 29–35.

Leung, H.W.C., Kuo, C.L., Yang, W.H., Lin, C.H., Lee, H.Z., 2006. Antioxidant enzymes activity involvement in luteolin-induced human lung squamous carcinoma CH27 cell apoptosis. Eur. J. Pharmacol. 534 (1), 12–18.

Majewska, M., Skrzycki, M., Podsiad, M., Czeczot, H., 2011. Evaluation of antioxidant potential of flavonoids: an in vitro study. Acta poloniae Pharm. 68 (4), 611.

Matławska, I. (Ed.). 2008. Pharmacognosy: a textbook for pharmacy students. University of Medical Sciences Ch.Marcinkowski.

Nasrollahzadeh, M., Sajadi, S.M., Rostami-Vartooni, A., Hussin, S.M., 2016. Green synthesis of CuO nanoparticles using aqueous extract of *Thymus vulgaris L.* leaves and their catalytic performance for N-arylation of indoles and amines. J. Colloid Interface Sci. 466, 113–119.

Obuchi, A., Ogata, A., Mizuno, K., Ohi, A., Ohuchi, H., 1993. Properties of Pd/Au and Pt/Cu alloy surface for the adsorption and catalytic reduction of O_2 and NO by H-2. Colloids Surf., A 80, 121–126.

Odenbrand, C.U.I., Blanco, J., Avila, P., Knapp, C., 1999. Learn NOx reduction in real diesel exhaust with copper and titaniabased monolithic catalyst. Appl. Catal. A Gen. 23, 37–44.

Otari, S.V., Yadav, H.M., Thorat, N.D., Patil, R.M., Lee, J.K., Pawar, S.H., 2016. Facile one pot synthesis of core shell Ag@ SiO_2 nanoparticles for catalytic and antimicrobial activity. Mater. Lett. 167, 179–182.

Rackauskas, S., Nasibulin, A.G., Jiang, H., Tian, Y., Kleshch, V.I., Sainio, J., Kauppinen, E.I., 2009. A novel method for metal oxide nanowire synthesis. Nanotechnology 20 (16), 165603.

Salata, O.V., 2004. Applications of nanoparticles in biology and medicine. J. Nanobiotechnol. 2 (1), 3.

Thandavarayan, M.X.D., Chen, P., Wang, X., 2012. Electrodeposited Pt on threedimensional interconnected graphene as a free-standing electrode for fuel cell application. J. Mater. Chem., 1–6 https://doi.org/10.1039/C2JM16541D.

Toshima, N., Wang, Y., 1994. Preparation and catalysis of novel colloidal dispersions of copper/noble metal bimetallic clusters. Langmuir 10, 4574–4580.

Valgas, C., Souza, S.M.D., Smânia, E.F., Smânia Jr, A., 2007. Screening methods to determine antibacterial activity of natural products. Braz. J. Microbiol. 38 (2), 369–380.

Xu, X., Qi, X., Wang, W., Chen, G., 2005. Separation and determination of flavonoids in *Agrimonia pilosa Ledeb.* by capillary electrophoresis with electrochemical detection. J. Separat. Sci. 28 (7), 647–652.

Zaleska-Medynska, A., Marchelek, M., Diak, M., Grabowska, E., 2016. Noble metal-based bimetallic nanoparticles: the effect of the structure on the optical, catalytic and photocatalytic properties. Adv. Colloid Interface Sci. 229, 80–107.

Zhong, C.J., Luo, J., Fang, B., Wanjala, B.N., Njoki, P.N., Loukrakpam, R., Yin, J., 2010. Nanostructured catalysts in fuel cells. Nanotechnology 21 (6), 062001.